



The effects of  
aerosols on water  
cloud

T. Michibata et al.

This discussion paper is/has been under review for the journal Atmospheric Chemistry and Physics (ACP). Please refer to the corresponding final paper in ACP if available.

# The effects of aerosols on water cloud microphysics and macrophysics based on satellite observations over East Asia and the North Pacific

T. Michibata<sup>1,3</sup>, K. Kawamoto<sup>2</sup>, and T. Takemura<sup>3</sup>

<sup>1</sup>Department of Earth System Science and Tech., Kyushu University, Fukuoka, Japan

<sup>2</sup>Graduate School of Fisheries Science and Environmental Studies, Nagasaki University, Nagasaki, Japan

<sup>3</sup>Research Institute for Applied Mechanics, Kyushu University, Fukuoka, Japan

Received: 16 March 2014 – Accepted: 14 April 2014 – Published: 28 April 2014

Correspondence to: T. Michibata (michibata@riam.kyushu-u.ac.jp)

Published by Copernicus Publications on behalf of the European Geosciences Union.

Title Page

Abstract

Introduction

Conclusions

References

Tables

Figures



Back

Close

Full Screen / Esc

Printer-friendly Version

Interactive Discussion



## Abstract

This study examines the characteristics of the microphysics and macrophysics of water clouds from East Asia to the North Pacific, using data from satellite observations. Our goals are to clarify differences in microphysics and macrophysics between land and oceanic clouds, seasonal differences unique to the mid-latitudes, characteristics of the drizzling process, and cloud vertical structure. In pristine oceanic areas, fractional occurrences of cloud optical thickness (COT) and cloud droplet effective radius (CDR) increase systematically with an increase in drizzle intensity, but in polluted land areas these characteristics of the COT and CDR transition are not as evident. Additionally, regional and seasonal differences are identified in terms of drizzle intensity as a function of the liquid water path (LWP) and cloud droplet number concentration ( $N_c$ ). The correlations between drizzle intensity and LWP, and between drizzle intensity and  $N_c$  are both more robust over oceanic areas than over land areas. We also demonstrate regional and seasonal characteristics of the cloud vertical structure. As a result, we find aerosol–cloud interaction mainly occurs around the cloud base in polluted land areas during the winter season. In addition, a difference between polluted and pristine areas in the efficiency of cloud droplet growth is confirmed. These results suggest that water clouds over the mid-latitudes exhibit a different drizzle system to those over the tropics.

## 1 Introduction

Aerosol particles play an important role in the climate system by serving as cloud condensation nuclei. The radiation budget is affected by their scattering and absorption properties, which are referred to as aerosol–radiation interactions. Additionally, aerosol–cloud interactions affect cloud optical thickness and cloud particle size (e.g., Twomey, 1977), and cloud lifetime (e.g., Albrecht, 1989). However, accurate and quantitative evaluation of these aerosol indirect effects is required to address the considerable uncertainty related to the heterogeneous nature of the spatial and temporal

### The effects of aerosols on water cloud

T. Michibata et al.

Title Page

Abstract

Introduction

Conclusions

References

Tables

Figures



Back

Close

Full Screen / Esc

Printer-friendly Version

Interactive Discussion



## The effects of aerosols on water cloud

T. Michibata et al.

Title Page

Abstract

Introduction

Conclusions

References

Tables

Figures

◀

▶

◀

▶

Back

Close

Full Screen / Esc

Printer-friendly Version

Interactive Discussion



distributions of aerosols. With respect to numerical models, many climate models have been developed and improved for accurate estimation of the global radiation balance. Practically all of the climate models, however, have uncertainty in their cloud precipitation parameterization schemes (e.g., Suzuki et al., 2013a) due to the difficulty of representing the complex aerosol–cloud interactions.

The cloud profiling radar (CPR) of CloudSat, whose mission began in 2006, may help clarify the details of cloud physical properties (Stephens et al., 2002), including vertical information that cannot be obtained from conventional satellite passive sensors, and is important to clarify aerosol indirect effects. Research on the physical properties of water clouds has advanced significantly in the last few years. Haynes and Stephens (2007) studied the relationships between cloud thickness and precipitation in the marine tropics, and found regional differences in the cloud vertical structure (shallow, middle, and deep modes) of precipitating clouds. Lebsock et al. (2008) investigated mainly aerosol–cloud interactions based on multi-sensor satellite observations, and found a relationship between variations in the cloud liquid water path (LWP) and the thermodynamic conditions. Kubar et al. (2009) compared the physical properties of water clouds in regions over tropical and subtropical oceans and stressed the importance of cloud macrophysics and microphysics to drizzle frequency and intensity. They also investigated which parameters were important to drizzle processes, focusing on macrophysics (cloud thickness and LWP) and microphysics (cloud droplet effective radius (CDR) and cloud droplet number concentration ( $N_c$ )). Nakajima et al. (2010) and Suzuki et al. (2010) attempted to visualize the vertical structure of cloud on a global scale using a method that they termed “contoured frequency by optical-depth diagram” (CFODD). Kawamoto and Suzuki (2012) applied CFODD to investigate precipitation process, and demonstrated that precipitation over the Amazon occurs in optically thicker locations than is the case over China.

Many researchers have investigated the physical structures and precipitation characteristics of low-level water clouds based on satellite observations. However, most of these studies have been limited to the tropics/sub-tropics or areas over oceans; only

a few have compared clouds over land and ocean. Very few have focused on East Asia, where some areas have significant levels of air pollution. Therefore clouds in these regions may exhibit drizzle characteristics that differ from those of clouds over tropical oceanic areas.

This study focuses on seasonal differences in water clouds that are characteristic of the mid-latitudes, and compares the characteristics of clouds over China (a region with considerable anthropogenic aerosols) with those over the North Pacific (a pristine area). We also analyze the transition processes of drizzle over both land and ocean in the mid-latitudes, which have been evaluated in only a few other studies.

## 2 Data and methodology

### 2.1 CloudSat

CloudSat was launched by the National Aeronautics and Space Administration (NASA) in 2006. It was the first project to include a spaceborne millimeter-wavelength (3 mm, frequency = 95 GHz) radar (Stephens et al., 2008) to help resolve the vertical structure of cloud droplets. We obtained information about cloud properties including the visible cloud optical thickness (COT) and CDR near the cloud top from the 2B-TAU product (Polonsky, 2008), and also radar reflectivity and the cloud mask from the 2B-GEOPROF product (e.g., Mace et al., 2007; Marchand et al., 2008). We used temperature and pressure data for each altitude from the ECMWF-AUX objective analysis (Partain, 2007). The analysis period was June, July, and August (JJA) from 2007–2009, and December, January, and February (DJF) from 2006–2009.

### 2.2 Regions and methods

Figure 1 shows maps of the regions investigated in this study. Inland includes the Gobi Desert; we select an area of Northeastern China (NE China) to study the effects of soil dust aerosols transported from the Gobi and Taklamakan deserts. Human activity

## The effects of aerosols on water cloud

T. Michibata et al.

Title Page

Abstract

Introduction

Conclusions

References

Tables

Figures



Back

Close

Full Screen / Esc

Printer-friendly Version

Interactive Discussion



## The effects of aerosols on water cloud

T. Michibata et al.

Title Page

Abstract

Introduction

Conclusions

References

Tables

Figures

◀

▶

◀

▶

Back

Close

Full Screen / Esc

Printer-friendly Version

Interactive Discussion



generates many anthropogenic aerosols in the Industrial area, and this region is one of the most air-polluted areas in the world (upper panel of Fig. 1). Some areas of Japan also discharge anthropogenic aerosols, but the main reason for selecting this region is to compare it with the Industrial area. We refer to the outflow regions of anthropogenic aerosols as North Pacific 1, 2, and 3 in order of their distance from East Asia. We investigated how large amounts of aerosols transported from East Asia affect cloud properties in these areas.

This study focuses only on low-level water clouds, because most aerosols remain in the lower troposphere. We define water clouds as those with a cloud mask value greater than 30, which means high-confidence detection, and a temperature above 273 K for the entire cloud layer. However, because few data meet these criteria in the Inland and NE China areas in DJF, we also include data for clouds with temperatures above 265 K, only in DJF in these two regions. Furthermore, we use only the data with uncertainty values of less than 3 and 1  $\mu\text{m}$  for COT and CDR, respectively. Multilayered clouds are excluded from the analyses to avoid ambiguous statistics.

### 3 Results

#### 3.1 Cloud physical properties for each area

Table 1 lists the physical properties of clouds over each of the seven areas. DJF values are given in parentheses. We used the following Eq. (1) to estimate  $N_c$  (e.g., Brenguier et al., 2000; Wood, 2006; Kubar et al., 2009),

$$N_c = \sqrt{2} B^3 \Gamma_{\text{eff}}^{1/2} \frac{\text{LWP}^{1/2}}{r^3} \quad (1)$$

where  $B = (3\pi\rho_w/4)^{1/3} = 0.0620$ , and  $\Gamma_{\text{eff}}$  is the adiabatic rate of increase in the liquid water content with height. Additionally, we calculated LWP by the following Eq. (2)

(Brenguier et al., 2000),

$$\text{LWP} = 5\tau_c r_e / 9 \quad (2)$$

where  $\tau_c$  and  $r_e$  were obtained from Moderate-resolution Imaging Spectroradiometer (MODIS) products. Lower tropospheric static stability (LTSS) is defined as the difference in potential temperatures between 700 hPa and the surface (Klein and Hartmann, 1993). This index was calculated from the ECMWF-AUX product (vertical temperature and pressure profiles).

Figure 2 shows the probability distribution function (PDF) of each cloud physical variable. The distribution of maximum radar reflectivity in the cloud layer ( $Z_{\max}$ ) (Fig. 2a) is similar for both the Industrial area and North Pacific 3, although we observe a slight shift to weaker  $Z_{\max}$  for the Industrial area. We confirm the tendency that smaller CDR values, larger  $N_c$  values, and optically thicker clouds are observed over land areas than over the oceanic regions in Fig. 2 and Table 1, supporting the findings of previous studies (e.g., Kawamoto et al., 2001). However, these results are not as obvious in the region over Japan as in other land areas, Inland, NE China, or the Industrial area. It is possible that the properties of clouds over NE China are affected in a complex manner by dust aerosols from the adjacent western deserts and emissions of anthropogenic aerosols from highly populated areas such as Beijing. The North Pacific 1 area has slightly larger values for COT, LWP, and  $N_c$  compared with the other oceanic areas, and the values of CDR are almost the same for all oceanic areas. Small seasonal differences are observed during JJA and DJF over the three oceanic areas; these differences are more obvious over the four land areas, which may be due to the high levels of aerosols in DJF, when atmospheric conditions are most stable.

The mode radii are approximately 15  $\mu\text{m}$  over the three oceanic areas, whereas they are approximately 9  $\mu\text{m}$  over the Industrial area in DJF, which may result in less efficient precipitation. The following subsections discuss how differences in the physical properties of clouds over land and ocean regions affect the rainfall characteristics.

The effects of aerosols on water cloud

T. Michibata et al.

Title Page

Abstract

Introduction

Conclusions

References

Tables

Figures

◀

▶

◀

▶

Back

Close

Full Screen / Esc

Printer-friendly Version

Interactive Discussion



## 3.2 COT–CDR diagram

COT and CDR are often considered to be typical cloud properties. The fact that the correlation between these parameters reflects cloud growth and precipitation processes has been well documented in previous studies based on satellite observations (e.g., Nakajima et al., 1991; Nakajima and Nakajima, 1995). Namely, both COT and CDR increase early in the growth process of cloud droplets, resulting in a positive correlation between them. The cloud particles grow to almost  $15\ \mu\text{m}$ , and precipitation begins. With precipitation, COT decreases and CDR increases due to coalescence. This precipitation process leads to a negative correlation pattern. Suzuki et al. (2006) extended these analyses, and successfully simulated the pattern using a spectral-bin microphysics model. Suzuki et al. (2011) documented fractional occurrences as a function of COT and CDR for each rain category (no precipitation, drizzle, and rain), and compared A-Train observations with model simulations.

Figure 3 shows fractional occurrences on COT–CDR diagrams for each rain category ([A] no precipitation;  $Z_{\text{max}} < -15$ , [B] drizzle;  $-15 \leq Z_{\text{max}} < 0$  and [C] rain;  $0 \leq Z_{\text{max}}$ ) (Comstock et al., 2004; Stephens and Haynes, 2007). The diagrams in the pristine remote ocean (North Pacific 3, Fig. 3g–l) reveal that the main group systematically shifts from the lower COT–CDR region to the higher COT–CDR region with an increase in the rain category (i.e., from no precipitation to rain), during both seasons. This tendency was also reported by Suzuki et al. (2011) and Kawamoto and Suzuki (2013). The fact that JJA (Fig. 3g–i) and DJF (Fig. 3j–l) have similar distributions suggests that the relation between COT and CDR has considerable universality with the rain categories over oceanic areas. However, in the Industrial area where air pollution by anthropogenic aerosols is severe, the transition pattern is not as clear as over the ocean. The category Rain in JJA (Fig. 3c) has relatively high values of fractional occurrence (approximately 0.2–0.5) in the small COT–CDR region ( $\text{COT} < 15$ ,  $\text{CDR} < 15\ \mu\text{m}$ ), while most values in this region (see Fig. 3i, l) are less than 0.2. Furthermore, we find that a large number of samples are concentrated in this region and that the cloud-top height in the Indus-

### The effects of aerosols on water cloud

T. Michibata et al.

[Title Page](#)[Abstract](#)[Introduction](#)[Conclusions](#)[References](#)[Tables](#)[Figures](#)[◀](#)[▶](#)[◀](#)[▶](#)[Back](#)[Close](#)[Full Screen / Esc](#)[Printer-friendly Version](#)[Interactive Discussion](#)

trial area is much higher (3.3 km) than that in the North Pacific 3 area (2.4 km). This finding suggests the existence of other predominant factors that affect drizzle intensity in the Industrial area during JJA, in addition to COT and CDR. Matsui et al. (2004) reported that not only the amount of aerosol but also the static stability was important for growth from cloud droplets into drizzle. The vertical inhomogeneity of CDR (larger particles appear in the lower part of clouds) is likely one reason for this. More analyses are required to clarify this issue further.

### 3.3 Transition pattern of precipitation

Some researchers have considered how the properties of clouds over land and ocean affect precipitation efficiency differently. Leon et al. (2008) analyzed CloudSat and Cloud-Aerosol Lidar and Infrared Pathfinder Satellite Observation (CALIPSO) data, and illustrated the global distribution of drizzle frequency as a function of LWP and CDR. We use  $N_c$  instead of CDR because we are focusing on differences in the amount of aerosol between land (polluted) and ocean (pristine) regions. Kubar et al. (2009) also investigated the drizzle frequency of water clouds over oceanic areas in the tropics and subtropics, as a function of a typical macrophysical variable (LWP) and a typical microphysical variable ( $N_c$ ). They found that the drizzle frequency increased with LWP when  $N_c$  was constant and decreased with increasing  $N_c$  and constant LWP. We focus on the mid-latitudes in the Northern Hemisphere, but more detailed analyses of mid-latitude regions would be valuable.

Figures 4 and 5 show the  $Z_{\max}$  distribution as a function of LWP and  $N_c$ , because we focus on the transition process of drizzle intensity rather than its frequency. Over three ocean regions (Figs. 4e–g and 5e–g), the drizzle intensity increases with increases LWP under a constant  $N_c$ , and increases with decreasing  $N_c$  under a constant LWP. It is important to clarify the physical parameters of clouds to understand the behavior of drizzle over the mid-latitudes as well as over the tropics/sub-tropics. Because the correlation coefficient  $r_1$  between LWP and  $Z_{\max}$  ( $\sim 0.6$ ) is greater than  $r_2$  between  $N_c$  and  $Z_{\max}$  ( $\sim -0.3$ ) in these areas, LWP has a stronger correlation than  $N_c$  with

## The effects of aerosols on water cloud

T. Michibata et al.

Title Page

Abstract

Introduction

Conclusions

References

Tables

Figures

◀

▶

◀

▶

Back

Close

Full Screen / Esc

Printer-friendly Version

Interactive Discussion



## The effects of aerosols on water cloud

T. Michibata et al.

Title Page

Abstract

Introduction

Conclusions

References

Tables

Figures

◀

▶

◀

▶

Back

Close

Full Screen / Esc

Printer-friendly Version

Interactive Discussion



drizzle intensity. This correlation is less clear over land areas than over oceanic areas, as shown in Figs. 4a–d and 5a–d. In particular, high values of  $Z_{\max}$  over the Industrial area are scattered during JJA because parameters other than LWP and  $N_c$  have strong effects on the drizzle transition process. This is consistent with our hypothesis that there is a more important dominant factor than cloud physical properties such as COT, CDR, LWP or  $N_c$  over the Industrial area in JJA. The seasonal difference is more obvious over the land areas than over the oceanic areas, with the magnitude of the correlation coefficients  $r_1$  and  $r_2$  being higher in DJF than in JJA. The land areas in JJA are in the unstable lower LTSS environment, with the exception of Japan. The low specific heat of the land surface would yield an unstable condition due to heating by stronger shortwave radiation in the JJA season. Such local heating may result in forced precipitation. We understand that the scattered distribution of high  $Z_{\max}$  values is caused by this. In addition, variations in the dynamics over land areas (e.g., vertical velocity) would also be associated with this seasonal difference.

Values of  $Z_{\max}$  greater than 0 dBZ<sub>e</sub> (orange and red in Figs. 4 and 5) are uncommon in the Inland and NE China areas during both JJA and DJF, which indicates very few precipitating clouds. In the Industrial area, there are some occasions when  $N_c$  is larger than 500 cm<sup>-3</sup>, and  $Z_{\max}$  values are lower as  $N_c$  becomes larger during DJF. Even LWP values, which are more strongly correlated with drizzle intensity, are larger. This finding suggests that the cloud lifetime increases due to water being stored inside the cloud layer. This finding is also observed in Japan (Fig. 5d), where a significant transition pattern appear as follows: LWP of 300 gm<sup>-2</sup> and  $N_c$  of 250 cm<sup>-3</sup>, to LWP of 450 gm<sup>-2</sup> and  $N_c$  of 100 cm<sup>-3</sup>, to LWP of 300 gm<sup>-2</sup> and  $N_c$  of 15 cm<sup>-3</sup>, as shown by the black arrows in Figs. 4d and 5d. LWP values increase to 400–500 gm<sup>-2</sup> as  $N_c$  values decrease because drizzle occurs only inside the cloud layer with no loss of water. At the same time, CDR values increase slowly within the range of 10–15 μm and then rapidly to larger values (15–25 μm), which leads to precipitation. The conditions in Japan are not as pristine as in the three oceanic regions, but are not as polluted as in the Industrial area, which is likely the reason for this V-shaped transition pattern.

### 3.4 Cloud vertical structure

Cloud geometrical thickness is a cloud macrophysical variable, in addition to the cloud-top height and LWP. Over the tropical ocean, cloud-top height corresponds to the cloud geometrical thickness, because the cloud base height is almost constant (e.g., Kubar et al., 2009). Cloud base height is, however, not always constant over mid-latitudes, in particular over the land; therefore, we use cloud geometrical thickness as a representative macrophysical variable. In fact, cloud geometrical thickness has a robust correlation with  $Z_{\max}$  (0.28–0.85; shown in Fig. 6), which is the index of precipitation intensity, rather than between cloud-top height and  $Z_{\max}$  (0.04–0.63).

The PDFs of cloud geometrical thickness are shown in Fig. 6. Solid (dotted) lines represent drizzling/precipitating (non-precipitating) cloud. The correlation between cloud geometrical thickness and  $Z_{\max}$  for JJA and DJF are denoted as  $r_{jja}$  and  $r_{djf}$ , respectively. Almost all of the non-precipitating clouds have less than 1000 m of geometrical thickness, and the clouds with precipitation are  $\sim 500$ –1000 m thicker. This trend and strong correlation between cloud geometrical thickness and  $Z_{\max}$  suggest the importance of cloud geometrical thickness for the occurrence of precipitation. The modal cloud geometrical thickness of the no-precipitation category is  $\sim 500$  m for the entire seven regions, during both seasons. On the other hand, the precipitating clouds have large seasonal variability. For instance, oceanic clouds (Fig. 6e–g) become thicker in DJF. Figure 7 is a histogram of cloud geometrical thickness for thin ( $< 800$  m; red), middle (800–2000 m; green), and thick ( $\geq 2000$  m; blue) clouds, which correspond roughly to no precipitation, drizzling, and precipitating clouds, respectively. The LTSS values listed in Table 1, which represent the air stability, tend to be consistent with the cloud geometrical thickness. More specifically, middle or thicker clouds exist predominantly in the unstable environment over the Industrial area in JJA (i.e., LTSS = 12.2 K). Conversely, in the stable environment in DJF (i.e., LTSS = 19.6 K), thinner clouds are more dominant. Similar to this tendency, the cloud geometrical thickness, which reflects the seasonal difference in LTSS, is also seen among other regions.

Title Page

Abstract

Introduction

Conclusions

References

Tables

Figures



Back

Close

Full Screen / Esc

Printer-friendly Version

Interactive Discussion



## The effects of aerosols on water cloud

T. Michibata et al.

Title Page

Abstract

Introduction

Conclusions

References

Tables

Figures

◀

▶

◀

▶

Back

Close

Full Screen / Esc

Printer-friendly Version

Interactive Discussion



Lebsock et al. (2008) confirmed that high-aerosol conditions tend to decrease LWP in nonprecipitating clouds, and the magnitude of the reduction in LWP is greater under the unstable low LTSS environment. These findings suggest the importance of LWP and thermodynamics to understanding aerosol–cloud interactions (L'Ecuyer et al., 2009).

We further investigate the cloud vertical structure, based on a comparison with the atmospheric conditions (pristine or polluted) associated with LWP and LTSS. Use of the CFODD to illustrate cloud vertical structure facilitates identification of associations with cloud optical properties, in particular, for single-layered water clouds (e.g., Nakajima et al., 2010; Suzuki et al., 2010). In general, the vertical and horizontal axes are allocated to geometrical height and radar reflectivity, respectively, when illustrating the frequency of the vertical radar profile. CFODD visualization methods apply the in-cloud optical depth (ICOD) as the vertical axis instead of altitude. In this way, normalization of the vertical coordinate by ICOD facilitates interpretation focusing on optical properties using composited clouds of different geometrical thicknesses. We obtained information on the layered optical depth from the 2B-TAU product.

CFODDs of each CDR bin ([A] 5–12  $\mu\text{m}$ , [B] 12–18  $\mu\text{m}$ , [C] 18–35  $\mu\text{m}$ ) over the Industrial area and North Pacific 3 are presented in Fig. 8. Although LTSS is correlated with cloud geometrical thickness, as we mentioned earlier, LTSS seems insensitive to the cloud growth process, because the values are almost identical among the three CDR bins. The CFODDs show that the LWP monotonically increases with increasing CDR, which corresponds to the transition from cloud particle (category [A]) to drizzle (category [B]), and raindrop (category [C]). In other words, CDR bin [A] represents evaporation and condensation processes, and CDR bins [B] and [C] represent mainly collision and coalescence processes. Therefore, an increase in LWP with an increase in CDR is expected. However, the rate of increase of LWP differs significantly between the Industrial area and North Pacific 3, as shown in Table 2. Namely, the rate of increase over North Pacific 3 is greater than that over the Industrial area. This result implies that the clouds over North Pacific 3 are more efficient than those over the Industrial area in terms of cloud droplet growth. Over the Industrial area in DJF, which is in the stable and





## The effects of aerosols on water cloud

T. Michibata et al.

Title Page

Abstract

Introduction

Conclusions

References

Tables

Figures

◀

▶

◀

▶

Back

Close

Full Screen / Esc

Printer-friendly Version

Interactive Discussion



a smaller rate of increase in LWP over polluted land. In addition, we found a difference in CFODD between the pristine oceanic area and the polluted land area, reflecting the aerosol–cloud interaction. To clarify these differences in cloud properties and drizzle characteristics between land and ocean, and between the tropics/sub-tropics and mid-latitudes, it is important to estimate the radiation budget accurately.

*Acknowledgements.* The CloudSat data products were provided by the CloudSat Data Processing Center at CIRA/Colorado State University. The authors would like to express their heartfelt gratitude to the CloudSat science team. This study was partly supported by the Funding Program for Next Generation World-Leading Researchers of the Cabinet Office, Government of Japan (GR079).

## References

- Albrecht, B. A.: Aerosols, cloud microphysics, and fractional cloudiness, *Science*, 245, 1227–1230, 1989. 10516, 10526
- Brenguier, J.-L., Pawlowska, H., Lothar, S., Rene, P., Jurgen, F., and Fouquart, Y.: Radiative properties of boundary layer clouds: droplet effective radius versus number concentration, *J. Atmos. Sci.*, 57, 803–821, 2000. 10519, 10520
- Comstock, K. K., Wood, R., Yuter, S. E., and Bretherton, C. S.: Reflectivity and rain rate in and below drizzling stratocumulus, *Quart. J. Roy. Meteor. Soc.*, 130, 2891–2918, doi:10.1256/qj.03.187, 2004. 10521
- Haynes, J. M. and Stephens, G. L.: Tropical oceanic cloudiness and the incidence of precipitation: early results from CloudSat, *Geophys. Res. Lett.*, 34, L09811, doi:10.1029/2007GL029335, 2007. 10517
- Kawamoto, K. and Suzuki, K.: Microphysical transition in water clouds over the Amazon and China derived from space-borne radar and radiometer data, *J. Geophys. Res.*, 117, D05212, doi:10.1029/2011JD016412, 2012. 10517
- Kawamoto, K. and Suzuki, K.: Comparison of water cloud microphysics over mid-latitude land and ocean using CloudSat and MODIS observations, *J. Quant. Spectrosc. Ra.*, 122, 13–24, doi:10.1016/j.jqsrt.2012.12.013, 2013. 10521

## The effects of aerosols on water cloud

T. Michibata et al.

Title Page

Abstract

Introduction

Conclusions

References

Tables

Figures

◀

▶

◀

▶

Back

Close

Full Screen / Esc

Printer-friendly Version

Interactive Discussion



- Kawamoto, K., Nakajima, T., and Nakajima, T. Y.: A global determination of cloud microphysics with AVHRR remote sensing, *J. Climate*, 14, 2054–2068, 2001. 10520
- Klein, S. A. and Hartmann, D. L.: The seasonal cycle of low stratiform clouds, *J. Climate*, 6, 1587–1606, 1993. 10520
- 5 Kubar, T. L., Hartmann, D. L., and Wood, R.: Understanding the importance of microphysics and macrophysics for warm rain in marine low clouds, Part I: Satellite observations, *J. Atmos. Sci.*, 66, 2953–2972, doi:10.1175/2009JAS3071.1, 2009. 10517, 10519, 10522, 10524
- Lebsock, M. D., Stephens, G. L., and Kummerow, C.: Multisensor satellite observations of aerosol effects on warm clouds, *J. Geophys. Res.*, 113, D15205, doi:10.1029/2008JD009876, 2008. 10517, 10525, 10527
- 10 L'Ecuyer, T. S., Berg, W., Haynes, J., Lebsock, M., and Takemura, T.: Global observations of aerosol impacts on precipitation occurrence in warm maritime clouds, *J. Geophys. Res.*, 114, D09211, doi:10.1029/2008JD011273, 2009. 10525
- Leon, D. C., Wang, Z., and Liu, D.: Climatology of drizzle in marine boundary layer clouds based on 1 year of data from CloudSat and Cloud-Aerosol Lidar and Infrared Pathfinder Satellite Observations (CALIPSO), *J. Geophys. Res.*, 113, D00A14, doi:10.1029/2008JD009835, 2008. 10522
- 15 Mace, G. G., Marchand, R., Zhang, Q., and Stephens, G.: Global hydrometeor occurrence as observed by CloudSat: initial observations from summer 2006, *Geophys. Res. Lett.*, 34, L09808, doi:10.1029/2006GL029017, 2007. 10518
- 20 Marchand, R., Mace, G. G., Ackerman, T., and Stephens, G.: Hydrometeor detection using CloudSat – an Earth-orbiting 94-GHz cloud radar, *J. Atmos. Ocean. Technol.*, 25, 519–533, doi:10.1175/2007JTECHA1006.1, 2008. 10518
- Matsui, T., Masunaga, H., Pielke Sr., R. A., and Tao, W.-K.: Impact of aerosols and atmospheric thermodynamics on cloud properties within the climate system, *Geophys. Res. Lett.*, 31, L06109, doi:10.1029/2003GL019287, 2004. 10522
- 25 Nakajima, T. Y. and Nakajima, T.: Wide-area determination of cloud microphysical properties from NOAA AVHRR measurements for FIRE and ASTEX regions, *J. Atmos. Sci.*, 52, 4043–4059, 1995. 10521
- 30 Nakajima, T., King, M. D., Spinhirne, J. D., and Radke, L. F.: Determination of the optical thickness and effective radius of clouds from reflected solar radiation measurements, Part II: Marine stratocumulus observations, *J. Atmos. Sci.*, 48, 728–750, 1991. 10521

## The effects of aerosols on water cloud

T. Michibata et al.

Title Page

Abstract

Introduction

Conclusions

References

Tables

Figures

◀

▶

◀

▶

Back

Close

Full Screen / Esc

Printer-friendly Version

Interactive Discussion



- Nakajima, T. Y., Suzuki, K., and Stephens, G. L.: Droplet growth in warm water clouds observed by the A-Train, Part II: A multisensor view, *J. Atmos. Sci.*, 67, 1897–1907, doi:10.1175/2010JAS3276.1, 2010. 10517, 10525, 10526
- 5 Nakatsuka, H., Kimura, T., Seki, Y., Kadosaki, G., Iide, Y., Okada, K., Yamaguchi, J., Takahashi, N., Ohno, Y., Horie, H., and Sato, K.: Design and development status of the Earth-CARE cloud profiling radar, *IEEE Int. Geosci. RemoteSensing Symp. (IGARSS)*, 2415–2418, doi:10.1109/IGARSS.2012.6351004, 22–27 July 2012. 10526
- Partain, P.: Cloudsat ECMWF-AUX auxiliary data process description and interface control document, Cooperative Institute for Research in the Atmosphere, Colorado State University, 10 pp., 2007. 10518
- Polonsky, I. N.: Level 2 cloud optical depth product process description and interface control document, Cooperative Institute for Research in the Atmosphere, Colorado State University, 21 pp., 2008. 10518
- 15 Schutgens, N. A. J.: Simulated Doppler radar observations of inhomogeneous clouds: application to the EarthCARE space mission, *J. Atmos. Ocean. Technol.*, 25, 26–42, doi:10.1175/2007JTECHA956.1, 2008. 10526
- Stephens, G. L. and Haynes, J. M.: Near global observations of the warm rain coalescence process, *Geophys. Res. Lett.*, 34, L20805, doi:10.1029/2007GL030259, 2007. 10521
- Stephens, G. L., Vane, D. G., Boain, R. J., Mace, G. G., Sassen, K., Wang, Z., Illingworth, A. J., O'Connor, E. J., Rossow, W. B., Durden, S. L., Miller, S. D., Austin, R. T., Benedetti, A., Mitrescu, C., and Team, T. C. S.: The Cloudsat mission and the A-Train, *B. Am. Meteorol. Soc.*, 83, 1771–1790, doi:10.1175/BAMS-83-12-1771, 2002. 10517
- 20 Stephens, G. L., Vane, D. G., Tanelli, S., Im, E., Durden, S., Rokey, M., Reinke, D., Partain, P., Mace, G. G., Austin, R., L'Ecuyer, T., Haynes, J., Lebsock, M., Suzuki, K., Waliser, D., Wu, D., Kay, J., Gettelman, A., Wang, Z., and Marchand, R.: CloudSat mission: performance and early science after the first year of operation, *J. Geophys. Res.*, 113, D00A18, doi:10.1029/2008JD009982, 2008. 10518
- Suzuki, K., Nakajima, T., Nakajima, T. Y., and Khain, A.: Correlation pattern between effective radius and optical thickness of water clouds simulated by a spectral bin microphysics cloud model, *Sola*, 2, 116–119, doi:10.2151/sola.2006-030, 2006. 10521
- 30 Suzuki, K., Nakajima, T. Y., and Stephens, G. L.: Particle growth and drop collection efficiency of warm clouds as inferred from joint CloudSat and MODIS observations, *J. Atmos. Sci.*, 67, 3019–3032, doi:10.1175/2010JAS3463.1, 2010. 10517, 10525, 10526

---

## The effects of aerosols on water cloud

T. Michibata et al.

---

Title Page

Abstract

Introduction

Conclusions

References

Tables

Figures

◀

▶

◀

▶

Back

Close

Full Screen / Esc

Printer-friendly Version

Interactive Discussion



Suzuki, K., Stephens, G. L., van den Heever, S. C., and Nakajima, T. Y.: Diagnosis of the warm rain process in cloud-resolving models using joint CloudSat and MODIS observations, *J. Atmos. Sci.*, 68, 2655–2670, doi:10.1175/JAS-D-10-05026.1, 2011. 10521, 10526

5 Suzuki, K., Stephens, G. L., and Lebsock, M. D.: Aerosol effect on the warm rain formation process: satellite observations and modeling, *J. Geophys. Res.*, 118, 170–184, doi:10.1002/jgrd.50043, 2013a. 10517

Suzuki, K., Golaz, J.-C., and Stephens, G. L.: Evaluating cloud tuning in a climate model with satellite observations, *Geophys. Res. Lett.*, 40, 4464–4468, doi:10.1002/grl.50874, 2013b. 10527

10 Sy, O. O., Tanelli, S., Takahashi, N., Ohno, Y., Horie, H., and Kollias, P.: Simulation of Earth-CARE spaceborne Doppler radar products using ground-based and airborne data: effects of aliasing and nonuniform beam-filling, *IEEE T. Geosci. Remote*, 52, 1463–1479, doi:10.1109/TGRS.2013.2251639, 2013. 10526

15 Twomey, S.: The influence of pollution on the shortwave albedo of clouds, *J. Atmos. Sci.*, 34, 1149–1152, 1977. 10516

Wood, R.: Relationships between optical depth, liquid water path, droplet concentration, and effective radius in adiabatic layer cloud, University of Washington, 3 pp., 2006. 10519

## The effects of aerosols on water cloud

T. Michibata et al.

**Table 1.** Cloud physical parameters in each area. JJA and DJF values are 3 year means. DJF values are in parentheses. Maximum values are shown in bold and minimum values are underlined. Maximum radar reflectivity in the cloud layer ( $Z_{\max}$ ) is used for precipitation categories (no precipitation;  $Z_{\max} < -15$ , drizzle;  $-15 \leq Z_{\max} < 0$ , rain;  $0 \leq Z_{\max}$ ).

	Land				Ocean		
	Inland	NE China	Industrial area	Japan	North Pacific 1	North Pacific 2	North Pacific 3
The number of samples	693 (139)	1315 (358)	3927 (4540)	11914 (10118)	20674 (15920)	25029 (17455)	<b>44064 (31949)</b>
$\tau_a$	0.29 (0.18)	0.40 (0.30)	<b>0.49 (0.44)</b>	0.23 (0.21)	0.24 (0.16)	0.17 (0.14)	0.14 (0.14)
$\tau_c$	22.2 (26.5)	<b>24.5 (28.4)</b>	19.5 ( <b>35.9</b> )	22.0 (26.3)	19.9 (21.5)	17.9 (19.4)	<u>16.4 (18.7)</u>
$r_e$ [ $\mu\text{m}$ ]	11.9 (9.7)	<u>11.9 (8.8)</u>	12.3 (10.5)	15.8 (14.5)	18.1 (17.8)	<b>18.5 (18.0)</b>	18.0 (17.3)
LWP [ $\text{g m}^{-2}$ ]	148 ( <u>136</u> )	161 (143)	<u>129 (205)</u>	189 (207)	<b>197 (215)</b>	185 (197)	167 (180)
$N_c$ [ $\text{cm}^{-3}$ ]	<b>154 (304)</b>	139 ( <b>338</b> )	125 (257)	77 (113)	51 (55)	42 ( <u>48</u> )	<u>41 (50)</u>
Maximum $Z_o$ [dBZ <sub>0</sub> ]	-5.8 (-10.4)	-8.1 (1.8)	<b>0.8 (-1.1)</b>	0.5 (0.9)	0.1 ( <b>2.0</b> )	-0.3 (0.7)	-1.5 (-1.2)
[%] with no precipitation	67.1 (55.4)	<b>70.5 (38.0)</b>	49.6 ( <b>61.5</b> )	46.2 (43.5)	<u>42.3 (35.3)</u>	43.3 (40.1)	46.4 (45.5)
[%] with drizzle	28.1 (44.6)	<u>26.5 (46.4)</u>	33.5 ( <u>29.1</u> )	34.0 (34.7)	<u>39.2 (38.5)</u>	<b>40.6 (38.5)</b>	40.5 (40.9)
[%] with rain	4.8 (0.0)	3.0 (15.6)	16.9 (9.4)	<b>19.8 (21.8)</b>	18.5 ( <b>26.2</b> )	16.1 (21.4)	13.1 (13.6)
Cloud-top height [km]	<b>3.7 (3.2)</b>	2.7 (2.0)	3.4 (2.3)	2.4 (2.4)	2.1 (2.2)	1.9 (2.0)	<u>1.8 (1.7)</u>
Geometrical thickness [km]	1.0 (0.8)	1.1 (1.0)	<b>1.2 (0.9)</b>	<b>1.2 (1.3)</b>	1.1 ( <b>1.3</b> )	1.0 (1.0)	<u>0.8 (0.8)</u>
LTSS [K]	13.8 (18.3)	15.2 (16.3)	<u>12.2 (19.6)</u>	16.5 (15.9)	<b>19.4 (15.8)</b>	18.3 (16.8)	18.2 (17.5)

[Title Page](#)
[Abstract](#)
[Introduction](#)
[Conclusions](#)
[References](#)
[Tables](#)
[Figures](#)
[Back](#)
[Close](#)
[Full Screen / Esc](#)
[Printer-friendly Version](#)
[Interactive Discussion](#)

## The effects of aerosols on water cloud

T. Michibata et al.

**Table 2.** LWP and its rate of increase for each CFODD.

	[A] $05 \leq \text{CDR} < 12 \mu\text{m}$	[B] $12 \leq \text{CDR} < 18 \mu\text{m}$	[C] $18 \leq \text{CDR} < 35 \mu\text{m}$
Industrial area			
JJA LWP [ $\text{g m}^{-2}$ ]	97.8	156.3	196.6
Rate of increase	1.60	1.26	1.35
DJF LWP [ $\text{g m}^{-2}$ ]			
JJA LWP [ $\text{g m}^{-2}$ ]	175.2	272.7	368.0
Rate of increase	1.56	1.35	1.35
North Pacific 3			
JJA LWP [ $\text{g m}^{-2}$ ]	69.1	140.8	222.7
Rate of increase	2.04	1.58	1.58
DJF LWP [ $\text{g m}^{-2}$ ]			
JJA LWP [ $\text{g m}^{-2}$ ]	97.8	156.5	245.1
Rate of increase	1.60	1.57	1.57

Title Page

Abstract

Introduction

Conclusions

References

Tables

Figures

◀

▶

◀

▶

Back

Close

Full Screen / Esc

Printer-friendly Version

Interactive Discussion



## The effects of aerosols on water cloud

T. Michibata et al.

Title Page

Abstract

Introduction

Conclusions

References

Tables

Figures

◀

▶

◀

▶

Back

Close

Full Screen / Esc

Printer-friendly Version

Interactive Discussion

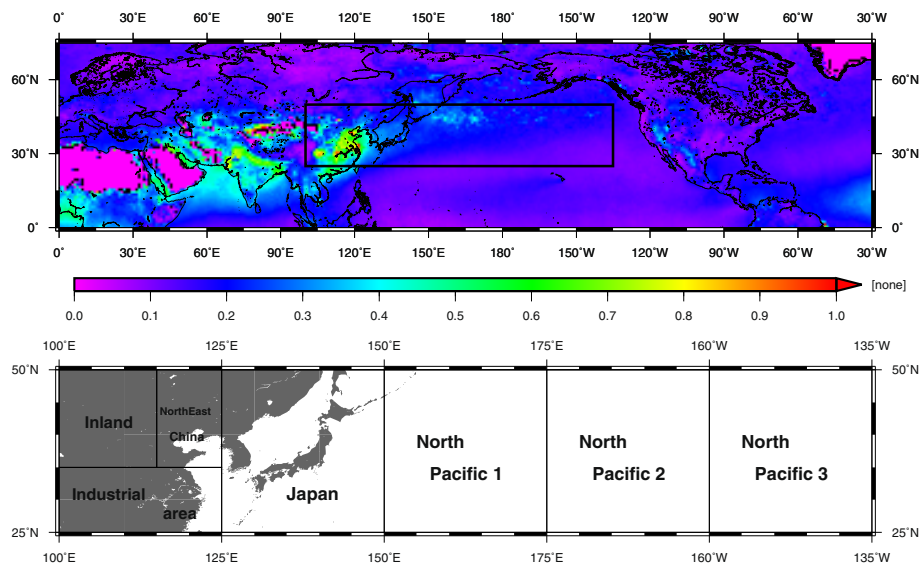


**Fig. 1.** Whole (top) and individual (bottom) regions in this study. Spatial distribution of aerosol optical thickness  $\tau_a$  (550 nm) for the 3 year mean derived from monthly Aqua/MODIS level 3 products are illustrated in the top panel.

## The effects of aerosols on water cloud

T. Michibata et al.

Title Page

Abstract

Introduction

Conclusions

References

Tables

Figures

◀

▶

◀

▶

Back

Close

Full Screen / Esc

Printer-friendly Version

Interactive Discussion

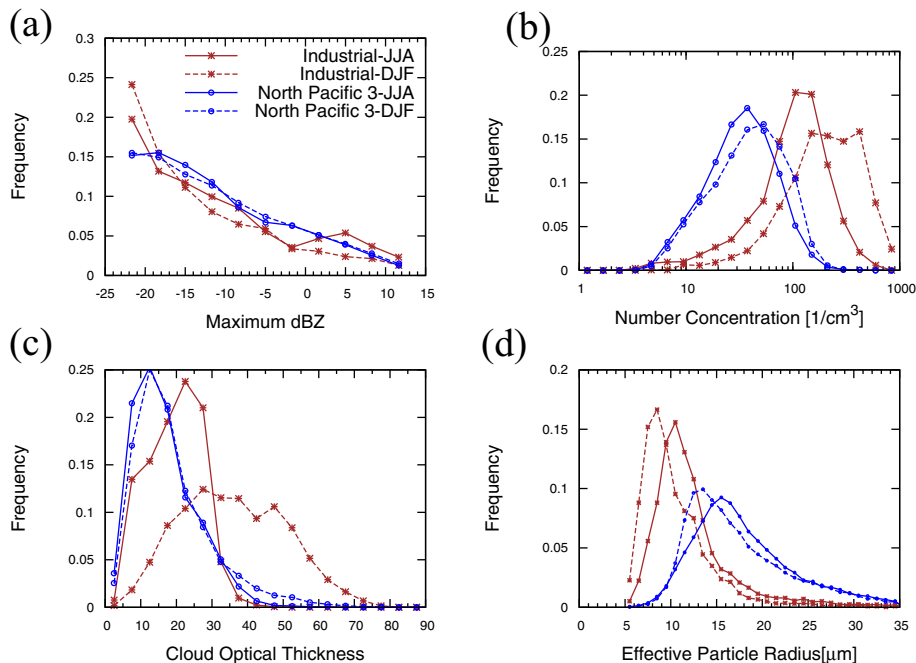


**Fig. 2.** Probability distribution functions of each cloud physical variable, **(a)** maximum radar reflectivity  $Z_{\max}$  [dBZ<sub>e</sub>], **(b)** cloud droplet number concentration  $N_c$  [cm<sup>-3</sup>], **(c)** cloud optical thickness  $\tau_c$ , and **(d)** cloud effective particle radius  $r_e$  [μm] for Industrial area and North Pacific 3 in JJA (solid line) and DJF (dotted line).

## The effects of aerosols on water cloud

T. Michibata et al.

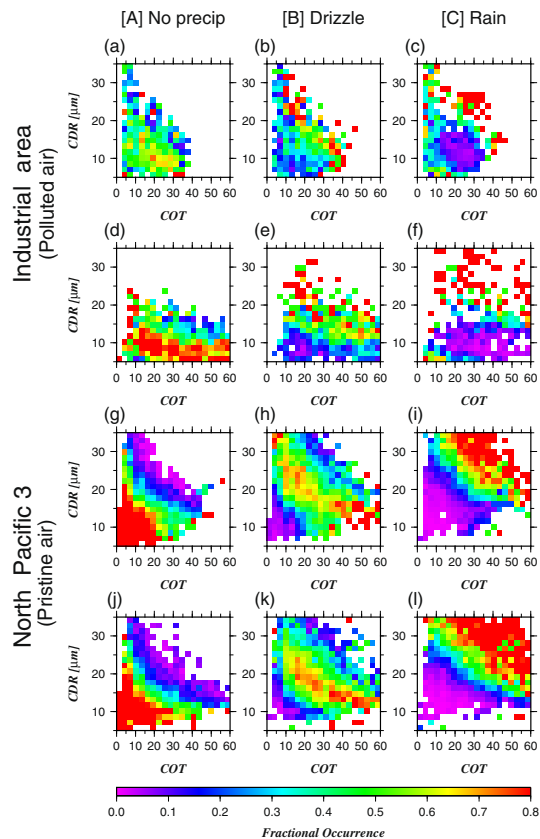


**Fig. 3.** Fractional occurrences of COT and CDR for each rain category: [A] no precipitation ( $Z_{\max} < -15$ ), [B] drizzle ( $-15 \leq Z_{\max} < 0$ ), and [C] rain ( $0 \leq Z_{\max}$ ). **(a–c)** are for the Industrial area in JJA, **(d–f)** for the Industrial area in DJF, **(g–i)** for the North Pacific 3 area in JJA, and **(j–l)** for the North Pacific 3 area in DJF.

## The effects of aerosols on water cloud

T. Michibata et al.

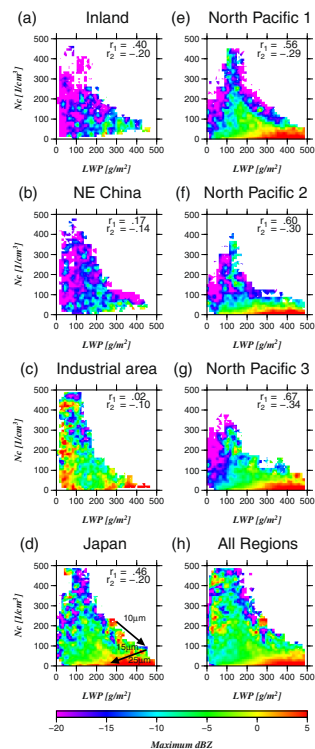


**Fig. 4.** Transition pattern of drizzle intensity during JJA (a) Inland, (b) NE China, (c) Industrial area, (d) Japan, (e) North Pacific 1, (f) North Pacific 2, (g) North Pacific 3, (h) the mean value of all regions.  $r_1$  is a correlation coefficient between LWP and  $Z_{\max}$  and  $r_2$  is a correlation coefficient between  $N_c$  and  $Z_{\max}$ .

## The effects of aerosols on water cloud

T. Michibata et al.

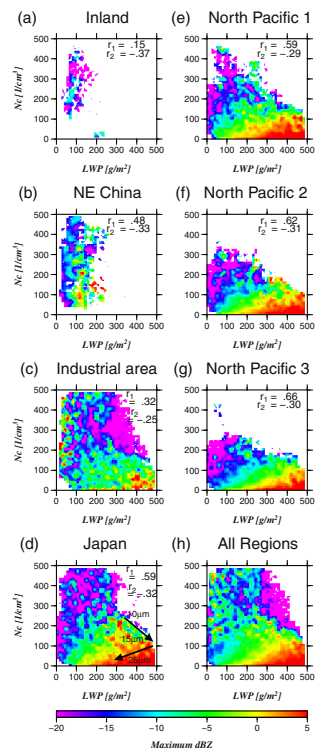


**Fig. 5.** Transition pattern of drizzle intensity during DJF (a) Inland, (b) NE China, (c) Industrial area, (d) Japan, (e) North Pacific 1, (f) North Pacific 2, (g) North Pacific 3, (h) the mean value of all regions.  $r_1$  is a correlation coefficient between LWP and  $Z_{\max}$  and  $r_2$  is a correlation coefficient between  $N_c$  and  $Z_{\max}$ .

The effects of aerosols on water cloud

T. Michibata et al.

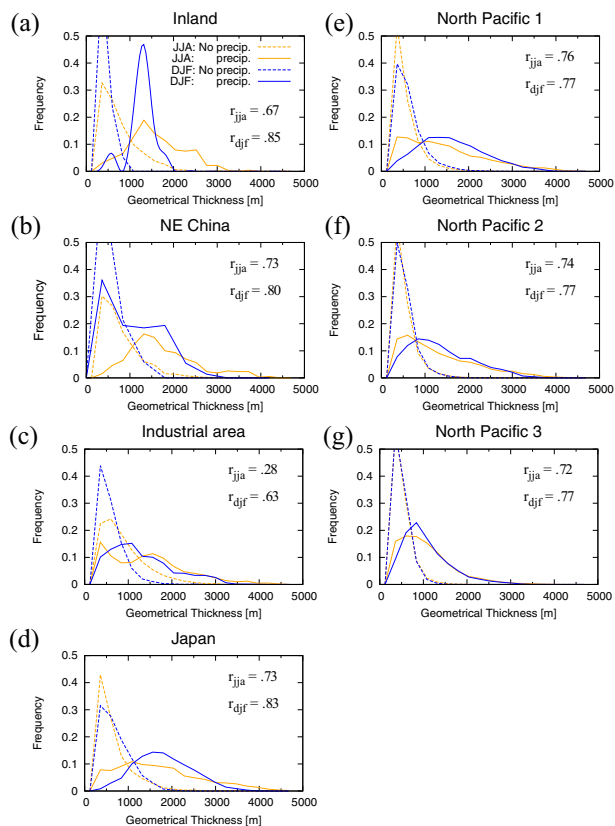


**Fig. 6.** Probability distribution functions of cloud geometrical thickness for nonprecipitating cloud (dotted line) and drizzling/precipitating cloud (solid line).  $r_{jja}$  is the correlation coefficient between cloud geometrical thickness and  $Z_{max}$  in JJA season, and  $r_{djf}$  is the same as  $r_{jja}$  but in the DJF season.

Title Page

Abstract

Introduction

Conclusions

References

Tables

Figures

◀

▶

◀

▶

Back

Close

Full Screen / Esc

Printer-friendly Version

Interactive Discussion





## The effects of aerosols on water cloud

T. Michibata et al.

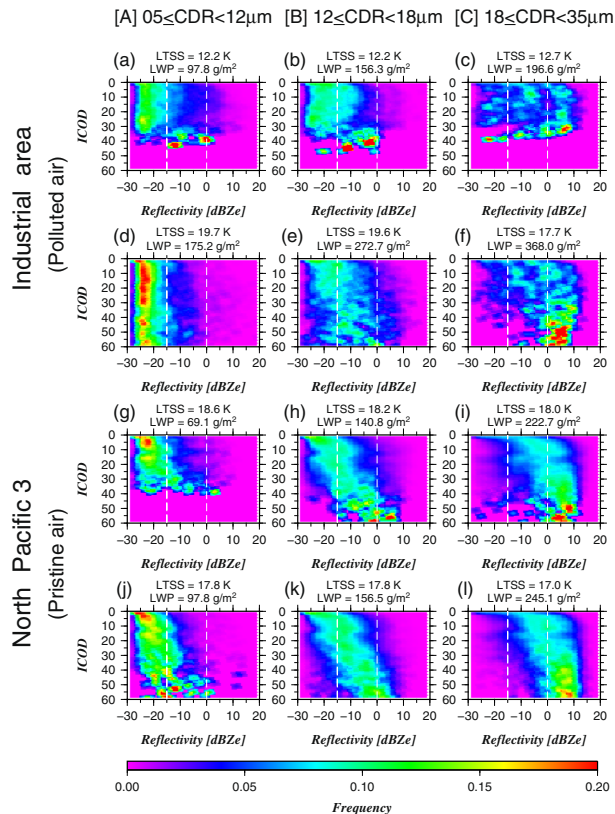


**Fig. 8.** CFODDs as a function of CDR, [A] 5–12  $\mu\text{m}$ , [B] 12–18  $\mu\text{m}$ , [C] 18–35  $\mu\text{m}$ . (a–c) are for the Industrial area in JJA, (d–f) for the Industrial area in DJF, (g–i) for the North Pacific 3 area in JJA, and (j–l) for the North Pacific 3 area in DJF. Two white dotted lines are drawn as threshold radar reflectivity values,  $-15 \text{ dBZ}_e$  and  $0 \text{ dBZ}_e$ , which are taken as the boundaries between cloud particles and drizzle, and between drizzle and rain, respectively. Averaged LWP and LTSS are also shown in each CFODD.